A Large Convective-Core Overshoot in *Kepler* Target KIC 11081729

Wuming YANG[1]

[1]Department of Astronomy, Beijing Normal University, Beijing 100875, China

*E-mail: yangwuming@bnu.edu.cn, yangwuming@ynao.ac.cn

Received ; Accepted

Abstract

The frequency ratios r_{01} and r_{10} of KIC 11081729 decrease firstly and then increase with the increase in frequency. For different spectroscopic constraints, all models with overshooting parameter $\delta_{\rm ov}$ less than 1.7 can not reproduce the distributions of the ratios. However, the distributions of the ratios can be directly reproduced by models with $\delta_{\rm ov}$ in the range of about $1.7-1.8$. The estimations of mass and age of the star can be affected by spectroscopic results, but the determination of the $\delta_{\rm ov}$ is not dependent on the spectroscopic results. A large overshooting of convective core may exist in KIC 11081729. The characteristics of r_{01} and r_{10} of KIC 11081729 may result from the effects of the large overshooting of convective core. The distributions of r_{01} and r_{10} of different stars with a convective core can be reproduced by the function $B(\nu_{n,1})$. If the value of the critical frequency ν_0 is larger than the value of frequency of maximum oscillation power ν_{max}, a star may have a small convective core and $\delta_{\rm ov}$. But if the value of ν_0 is less than that of ν_{max}, the star may have a large convective core and $\delta_{\rm ov}$. The function aids in determining the presence of convective core and the size of the convective core including overshooting region from observed frequencies. The determination is not dependent on the calculation of stellar models.

Key words: stars: evolution – stars: interiors – stars: oscillations.

1 Introduction

Asteroseismology has proved to be a powerful tool for determining the fundamental parameters of stars, diagnosing the internal structure of stars, and probing physical processes in stellar interiors by comparing observed oscillation characteristics with those calculated from theoretical models (Mazumdar et al. 2006; Cunha & Metcalfe 2007; Christensen-Dalsgaard & Houdek 2010; Yang et al. 2012; Silva Aguirre et al. 2013; Liu et al. 2014; Guenther et al. 2014; Chaplin et al. 2014; Metcalfe et al. 2014; Tian et al. 2014).

However, the stellar model found solely by matching individual frequencies of oscillation does not always properly reproduce other characteristics of oscillations (Deheuvels et al. 2010; Silva Aguirre et al. 2013; Liu et al. 2014), such as the ratios of small-to-large separations, r_{10} and r_{01}, which are sensitive to conditions in stellar core (Roxburgh & Vorontsov 2003). The small separations are defined as (Roxburgh & Vorontsov 2003)

$$d_{10}(n) \equiv -\frac{1}{2}(-\nu_{n,0} + 2\nu_{n,1} - \nu_{n+1,0}) \tag{1}$$

and

$$d_{01}(n) \equiv \frac{1}{2}(-\nu_{n,1} + 2\nu_{n,0} - \nu_{n-1,1}). \tag{2}$$

In calculation, equations (1) and (2) are rewritten as the smoother five-point separations.

Stars with a mass larger than $1.1\ M_{\odot}$ may have a convective core during their main sequence (MS). The overshooting of the convective core extends the region of material mixing by a distance $\delta_{\rm ov}$ H_p above the top of the convective core that is determined by Schwarzchild criterion, where H_p is the local pressure scale-height and $\delta_{\rm ov}$ is a free parameter. The overshooting brings more H-rich material into the core, prolongs the lifetime of the burning of core hydrogen, and changes the internal structure of stars and the global characteristics of the following giant stages (Schröder et al. 1997; Yang et al. 2012). The determination of the global parameters of stars by asteroseismology or other studies based on stellar evolution can be directly affected by the overshooting (Mazumdar et al. 2006; Yang et al. 2012).

However, for stars with a mass of around $1.1\ M_{\odot}$, there may or may not exist a convective core in their interior, depending on the input physics used in the computation of their evolutions (Christensen-Dalsgaard & Houdek 2010). Up to now, there is no a direct method to determine the presence and the size of the convective core and the extension of overshooting from observed data. Therefore, finding a method of determining the presence and the size of the convective core is important for understanding the structure and evolution of stars.

Deheuvels et al. (2010) argued that the presence or absence of a convective core in stars can

be indicated by the small separations and that the star HD 203608 with $M \simeq 0.94\ M_{\odot}$ and $t \simeq 6.7$ Gyr in fact has a convective core. De Meulenaer et al. (2010) studied the oscillations of α Centauri A ($1.105 \pm 0.007\ M_{\odot}$) and concluded that the d_{01} allows them to set an upper limit to the amount of convective-core overshooting and that the model of α Centauri A with a radiative core reproduces the observed r_{01} significantly better than the model with a convective core. Moreover, Silva Aguirre et al. (2013) tried to detect the convective core of KIC 6106415 and KIC 12009504. They obtained that the mass of KIC 6106415 is $1.11 \pm 0.05\ M_{\odot}$ and that of KIC 12009504 is $1.15 \pm 0.04\ M_{\odot}$, and concluded that a convective core and core overshooting exist in KIC 12009504, but could not determine whether a convective core exists in KIC 6106415. Tian et al. (2014) studied the oscillations of KIC 6225718 and concluded that either a small convective core or no convective core exists in the star.

For MS stars, the ratios generally decrease with frequency. Liu et al. (2014) argued that the ratios affected by the overshooting of convection core could exhibit an increase behavior. By using this seismic tool, the value of overshooting parameter $\delta_{\rm ov}$ is restricted between 0.4 and 0.8 for HD 49933 (Liu et al. 2014) and between 1.2 and 1.6 for KIC 2837475 (Yang et al. 2015). Moreover, Guenther et al. (2014) found that the value of $\delta_{\rm ov}$ is between 0.9 and 1.5 for Procyon, which is supported by the work of Bond et al. (2015). The values of $\delta_{\rm ov}$ are larger than the value of $0.1 - 0.3$ estimated by comparing the theoretical and observational color-magnitude diagram of star clusters (Prather & Demarque 1974; Demarque et al. 1994) and characteristics of eclipsing binary stars (Schröder et al. 1997).

However, the presence of the large overshooting is supported by the convective theory of stars and numerical simulation. For example, Xiong (1985) shows that if the overshooting distance is defined as the distance up to which mixing of matter extends, the overshooting distance of the convective core can reach $1.4c_1\ H_p$ in his convective theory, where the value of the c_1 is between $1/3$ and 1; the numerical simulation of Tian et al. (2009) shows that the penetration distance of downward overshooting of convection of giant stars can reach $1 - 2\ H_p$. Moreover, Valle et al. (2016) show that the calibration of the convective core overshooting of double-lined eclipsing binaries with the mass in the range of $1.1 - 1.6\ M_{\odot}$ is poorly reliable. They suggested that asteroseismic data may be required for the calibration of $\delta_{\rm ov}$.

KIC 11081729 is an F5 star (Wright et al. 2003). The frequencies of p-modes of KIC 11081729 have been extracted by Appourchaux et al. (2012). Combing asteroseismical and non-asteroseismical data, several authors (Huber et al. 2014; Metcalfe et al. 2014) have investigated the fundamental parameters of KIC 11081729. The mass determined by Huber et al. (2014) is $1.36^{+0.04}_{-0.06}$ $M_{\odot}$ for KIC 11081729, but that determined by Metcalfe et al. (2014) is $1.26 \pm 0.03\ M_{\odot}$. The observed ratios r_{10} and r_{01} of KIC 11081729 decrease firstly and then increase with the increase in frequencies.

The characteristics may derive from the effects of overshooting of convective core. If these characteristics can be directly reproduced by stellar models, which may aid in understanding the origin of the characteristics and confirming the presence of the large overshooting of convective core.

In this work, we focus mainly on examining whether the observed characteristics of KIC 11081729 can be directly reproduced by stellar models and can be explained by overshooting of convective core. In order to find the best model of KIC 11081729, the chi squared method was used. First, an approximate set of models was found out with the constraints of luminosity, $T_{\rm eff}$, and [Fe/H]. Then around this set of solutions, we sought for best models that match both non-seismic constraints and the individual frequencies extracted by Appourchaux et al. (2012), and then we compared the observed r_{10} and r_{01} with those calculated from models. And finally, a function $B(\nu_{n,1})$ was deduced and tested. In Section 2, stellar models of KIC 11081729 are introduced. In Section 3, the function $B(\nu_{n,1})$ is deduced, and in Section 4, the results are summarized and discussed.

2 STELLAR MODELS

2.1 Input Physics

In order to obtain the best model of KIC 11081729, we construct a grid of evolutionary models using the Yale Rotation Evolution Code (YREC) (Pinsonneault et al. 1989; Yang & Bi 2007). For the microphysics, the OPAL equation-of-state table EOS2005 (Rogers & Nayfonov 2002), OPAL opacity table GN93 (Iglesias & Rogers 1996), and the low-temperature opacity tables of Alexander & Ferguson (1994) are used. The standard mixing-length theory is adopted to treat convection. The value of the mixing-length parameter α calibrated to the Sun is 1.74 for the YREC. But it is a free parameter in this work. The full mixing of material is assumed in overshooting region of models. The diffusion and settling of both helium and heavy elements are taken into account in models with a mass less than 1.30 $M_{\odot}$ by using the diffusion coefficients of Thoul et al. (1994). In the model calculation, the initial helium mass fraction is fixed at 0.248 and 0.295. The value of 0.248 is the standard big bang nucleosynthesis value (Spergel et al. 2007). The values of input parameters, mass (M), α and $\delta_{\rm ov}$, and heavy-element abundance (Z) of Zero-Age MS models are listed in Table 1. The models are constructed from ZAMS to the end of MS or the subgiant stage. Some of evolutionary tracks of the models are shown in Figure 1 as an example.

The low-l p-mode frequencies of each model are calculated by using the Guenther's adiabatic oscillation code (Guenther 1994). For the modes with a given degree l, the frequencies $\nu_{\rm corr}(n)$ corrected from the near-surface effects of the model are computed by using equation (Kjeldsen et al. 2008)

Table 1. Input parameters for model tracks. The symbol δ indicates the resolution of the parameters.

Variable	Minimum	Maximum	δ
M/M$_\odot$	1.01	1.50	$\leq$0.02
α	1.65	2.15	0.1
$\delta_{\rm ov}$	0.0	1.8^a	0.2
Z_i	0.010	0.040	0.002

^{a} Supplemented by $\delta_{\rm ov}$ = 1.7.

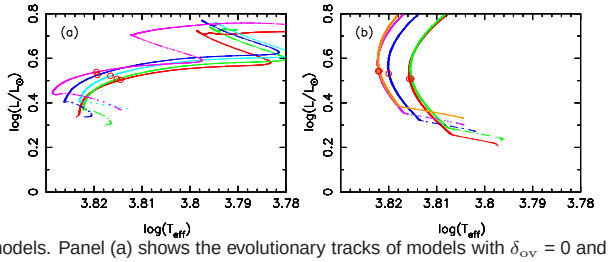

Fig. 1. Hertzsprung-Russell diagram of models. Panel (a) shows the evolutionary tracks of models with $\delta_{\rm ov}$ = 0 and 0.2 with the spectroscopic constraints of Bruntt et al. (2012), while panel (b) depicts those of models with $\delta_{\rm ov}$ = 1.8. The circles indicate the most likely models for KIC 11081729.

$$\nu_{\rm corr}(n) = \nu_{\rm mod}(n) + a[\frac{\nu_{\rm mod}(n)}{\nu_{max}}]^b, \tag{3}$$

where b is fixed to be 4.9, a is a parameter, $\nu_{\rm mod}(n)$ is the adiabatic oscillation frequencies of the model, $\nu_{\rm max}$ is the frequency of maximum power. The value of $\nu_{\rm max}$ is 1820 μHz. The value of a is determined from the observed and theoretical frequencies of the modes with the degree l by using equations (6) and (10) of Kjeldsen et al. (2008).

2.2 Spectroscopic Constraints

The effective temperature of KIC 11081729 may be 6440 K (Wright et al. 2003), 6570^{+67}_{-75} K (Ammons et al. 2006), 6359 K (Pinsonneault et al. 2012), 6630 ± 70 K (Bruntt et al. 2012), or 6400 ± 127 K (Molenda-Zakowicz et al. 2013). The value of [Fe/H] for KIC 11081729 is $0.16^{+0.14}_{-0.15}$ (Ammons et al. 2006). Combining the value of $(Z/X)_\odot = 0.023$ of the Sun given by Grevesse & Sauval (1998), the ratio of surface metal abundance to hydrogen abundance, $(Z/X)_{\rm s}$, is estimated to be approximately between 0.024 and 0.047. The value of [Fe/H] determined by Bruntt et al. (2012) is -0.12 ± 0.06, which corresponds to a $(Z/X)_{\rm s}$ approximately between 0.015 and 0.020; while that estimated by Molenda-Zakowicz et al. (2013) is -0.19 ± 0.22, i.e., the value of $(Z/X)_{\rm s}$ is approximately between 0.009 and 0.025. Molenda-Zakowicz et al. (2013) have shown that the estimated atmospheric parameters of stars hotter than 6,000 K are affected by the method of spectral analysis. Thus the atmospheric parameters determined by Ammons et al. (2006), Bruntt et al. (2012), and Molenda-Zakowicz et al.

(2013) were considered in this work.

The visual magnitude of KIC 11081729 is 9.048 ± 0.054 (Droege et al. 2006; Ammons et al. 2006). The value of bolometric correction and extinction is estimated from the tables of Flower (1996) and Ammons et al. (2006), respectively. The distance of KIC 11081729 is $D = 99^{+91}_{-36}$ pc (Ammons et al. 2006; Pickles & Depagne 2010). Then the luminosity of KIC 11081729 is estimated to be $4.00 \pm 3.28\ L_{\odot}$. The large uncertainty of the luminosity derives from the uncertainty of the distance.

To find the models that can reproduce the observed characteristics of KIC 11081729, we calculated the value of $\chi^2_{\rm c}$ of models. The function $\chi^2_{\rm c}$ is defined as

$$\chi^2_{\rm c} = \frac{1}{3}\sum_{i=1}^{3}[\frac{C_i^{\rm theo} - C_i^{\rm obs}}{\sigma(C_i^{\rm obs})}]^2, \tag{4}$$

where the symbol $C = [L/L_{\odot}, T_{\rm eff}, (Z/X)_s]$, the $C_i^{\rm obs}$ presents the observed values of these parameters, while $C_i^{\rm theo}$ represents the theoretical values. The observational error is given by $\sigma(C_i^{\rm obs})$. In the first step, the models with $\chi^2_{\rm c} \leq 1$ are chosen as candidate models.

2.3 Asteroseismic Constraints

In order to find the models that can reproduce the oscillation characteristics of KIC 11081729, we computed the value of χ^2_{ν} for each model. The function χ^2_{ν} is defined as

$$\chi^2_{\nu} = \frac{1}{N}\sum_{i=1}^{N}[\frac{\nu_i^{\rm theo} - \nu_i^{\rm obs}}{\sigma(\nu_i^{\rm obs})}]^2, \tag{5}$$

where the quantity ν corresponds to the individual frequencies of modes from observation and modelling, $\sigma(\nu_i^{\rm obs})$ is the observational error of the $\nu_i^{\rm obs}$, N presents the number of observed modes. The value of $\chi^2_{\nu_{\rm corr}}$ of corrected frequencies is also computed. The models with $\chi^2_{\rm c} \leq 1.0$ and χ^2_{ν} or $\chi^2_{\nu_{\rm corr}}$ < 10.0 are chosen as candidate models.

When a model evolves to the vicinity of the error-box of $L/L_{\odot}$ and $T_{\rm eff}$ in the H-R diagram, the evolutionary time step of the model is set as small as possible to ensure that consecutive models have an approximately equal $\chi^2_{\nu_{\rm corr}}$. In some cases, there may be a difference of a few Myr between the age of the model with the minimum $\chi^2_{\nu_{\rm corr}}$ and that of the model with the minimum χ^2_{ν}. Yang et al. (2015) showed that the difference between the model with the minimum $\chi^2_{\nu_{\rm corr}}$ and the model with the minimum χ^2_{ν} is insignificant. For a given mass and $\delta_{\rm ov}$, the model with the minimum $\chi^2_{\nu_{corr}}$ is chosen as the best model.

Table 2. Parameters of the models with the effective temperture and [Fe/H] determined by Bruntt et al. (2012). The symbol X_c represents the central hydrogen abundance of models, while ν_0^m indicates the adiabatic oscillation frequency at which the r_{01} of models reaches a minimum.

Model	M ($M_\odot$)	$T_{\rm eff}$ (K)	L ($L_\odot$)	R ($R_\odot$)	age (Gyr)	Z_i	$(Z/X)_s$	α	$\delta_{\rm ov}$	X_c	χ^2_ν	$\chi^2_{\nu_{corr}}$	χ^2_c	ν_0^m (μHz)
Mb1	1.21	6524	3.19	1.400	2.475	0.018	0.018	2.05	0.2	0.410	5.5	5.6	0.8	2255
Mb2	1.22	6524	3.20	1.403	2.488	0.018	0.017	2.05	0.2	0.417	5.9	5.5	0.8	2255
Mb3	1.23	6534	3.22	1.403	2.222	0.018	0.016	1.95	0.2	0.450	5.9	5.6	0.9	2346
Mb4	1.24	6556	3.27	1.403	2.073	0.018	0.015	1.95	0.2	0.461	6.6	5.5	0.7	2347
Mb5	1.25	6596	3.35	1.403	1.856	0.018	0.014	1.95	0.2	0.479	7.1	5.3	0.6	2347
Mb6	1.26	6641	3.47	1.409	1.835	0.018	0.015	2.05	0.2	0.476	6.1	5.4	0.4	2347
Mb7	1.27	6555	3.33	1.416	1.907	0.020	0.018	1.95	0.2	0.478	5.4	5.2	0.4	2347
Mb8	1.28	6583	3.39	1.416	1.750	0.020	0.017	1.95	0.2	0.492	7.1	5.3	0.2	2347
Mb9	1.29	6599	3.46	1.426	1.697	0.020	0.019	2.05	0.0	0.389	4.9	5.4	0.1	3562
Mb10	1.30	6553	3.40	1.432	2.452	0.016	0.022	1.95	0.0	0.327	5.5	5.5	0.9	4010

2.3.1 The models with the effective temperature and [Fe/H] of Bruntt

With the constraints of the effective temperature and the [Fe/H] of Bruntt et al. (2012), we calculated the values of $\chi^2_{\rm c}$, χ^2_ν, and $\chi^2_{\nu_{\rm corr}}$ of each model. Table 2 lists the models that minimize $\chi^2_{\rm c}$ + $\chi^2_{\nu_{\rm corr}}$ for a given mass. The value of $\delta_{\rm ov}$ of the models is less than 0.4. The model Mb8 has the minimum $\chi^2_{\rm c}$ + $\chi^2_{\nu_{\rm corr}}$, which seems to hint that Mb8 is the best model.

Using the posterior probability distribution function, the mass estimated from the sample of the models with $\chi^2_{\rm c} < 1.0$ and $\chi^2_{\nu_{\rm corr}} < 10.0$ is $1.26 \pm 0.03\ M_\odot$ for KIC 11081729, where the error bar indicates the 68% level confidence interval. With the same constraints, Metcalfe et al. (2014) also obtained the same mass, i.e. $1.26 \pm 0.03\ M_\odot$. The radius is estimated to be $1.41 \pm 0.01\ R_\odot$ that is also close to $1.382 \pm 0.021\ R_\odot$ of Metcalfe et al. (2014). However, the age of 1.9 ± 0.4 Gyr is larger than 0.86 ± 0.21 Gyr given by Metcalfe et al. (2014). This is due to the fact that the effects of the settling of heavy elements and overshooting of convective core were considered that were not included in the models of Metcalfe et al. (2014). This indicates that the estimated age of stars can be significantly affected by physical effects that are considered in models.

However, the calculations show that the models with $\delta_{\rm ov} \leq 0.2$ can not reproduce the distributions of the observed r_{10} and r_{01} of KIC 11081729 (see Figure 2). This shows that the internal structures of these models do not match that of KIC 11081729. The observed ratios change dramat-

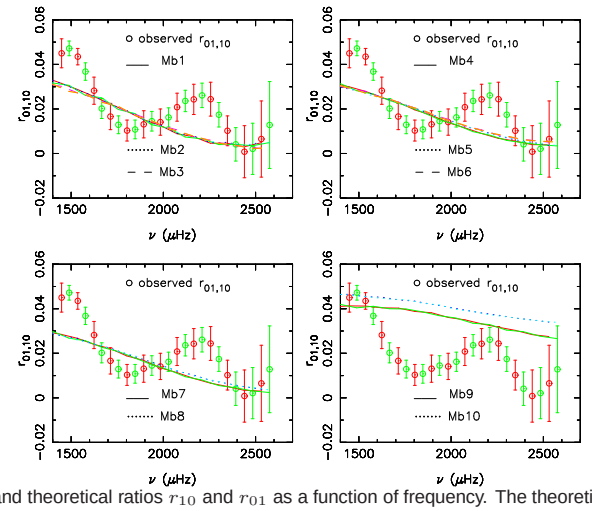

Fig. 2. The distributions of the observed and theoretical ratios r_{10} and r_{01} as a function of frequency. The theoretical ratios are computed from the corrected oscillation frequencies $\nu_{\rm corr}$ of the models listed in Table 2.

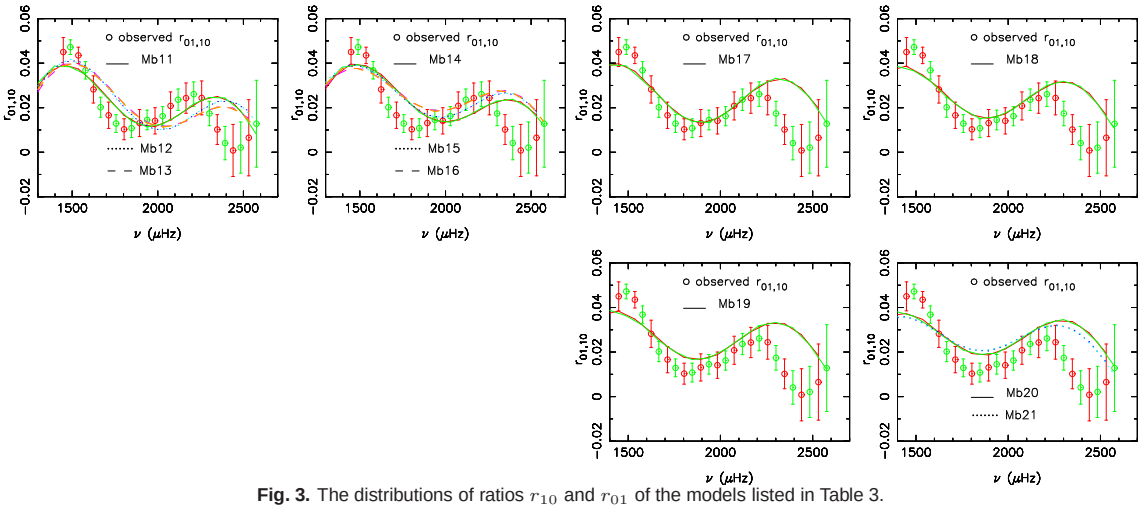

Fig. 3. The distributions of ratios r_{10} and r_{01} of the models listed in Table 3.

ically at high frequencies, which may derive from the fact that the observed frequencies are affected by large-line widths at high frequencies in the same way as that of KIC 6106415 and KIC 12009504 (Silva Aguirre et al. 2013). Silva Aguirre et al. (2013) suggested that the ratios at high frequencies should be excluded from the set of constraints.

Liu et al. (2014) argued that effects of overshooting of convective core can lead to the fact that ratios r_{10} and r_{01} exhibit an increase behavior. In order to test whether the characteristics of r_{10} and r_{01} of KIC 11081729 can be reproduced by the effects of overshooting, we computed the evolutions of models with $\delta_{\rm ov}$ as large as 1.8. The calculation shows that models with $\delta_{\rm ov} < 1.7$ can not reproduce the distributions of the observed r_{10} and r_{01}. Table 3 lists the models that minimize $\chi^2_{\rm c}$ + $\chi^2_{\nu_{\rm corr}}$ for a given mass and $\delta_{\rm ov}$. Model Mb19 has the minimum $\chi^2_{\rm c}$ + $\chi^2_{\nu_{\rm corr}}$. Moreover, Figure 3 shows that the observed ratios can be reproduced well by models with $\delta_{\rm ov} = 1.8$ and mass in the range of $1.21 - 1.27$ $M_{\odot}$.

Table 3. Parameters of the models with the effective temperture and [Fe/H] determined by Bruntt et al. (2012). The symbol X_c represents the central hydrogen abundance of models, while ν_0^m indicates the adiabatic oscillation frequency at which the r_{01} of models reaches a minimum.

Model	M ($M_\odot$)	$T_{\rm eff}$ (K)	L ($L_\odot$)	R ($R_\odot$)	age (Gyr)	Z_i	$(Z/X)_s$	α	$\delta_{\rm ov}$	X_c	χ^2_ν	$\chi^2_{\nu_{corr}}$	χ^2_c	ν_0^m (μHz)
Mb11	1.19	6560	3.19	1.384	4.415	0.020	0.015	1.95	1.7	0.566	20.8	8.9	0.8	818
Mb12	1.21	6529	3.20	1.400	4.567	0.024	0.020	2.05	1.7	0.557	10.6	8.1	0.9	818
Mb13	1.23	6605	3.36	1.400	3.793	0.022	0.017	2.05	1.7	0.574	13.7	8.0	0.1	817
Mb14	1.25	6596	3.38	1.409	3.603	0.024	0.019	2.05	1.7	0.576	12.4	7.4	0.2	817
Mb15	1.27	6585	3.40	1.419	3.426	0.026	0.022	2.05	1.7	0.579	9.8	7.0	0.7	817
Mb16	1.29	6582	3.40	1.419	2.856	0.026	0.021	1.95	1.7	0.594	14.4	7.5	0.4	816
Mb17	1.21	6542	3.22	1.400	4.631	0.024	0.020	2.05	1.8	0.559	10.8	7.8	0.7	818
Mb18	1.23	6536	3.22	1.403	4.000	0.024	0.019	1.95	1.8	0.574	14.9	7.7	0.6	817
Mb19	1.25	6607	3.40	1.409	3.654	0.024	0.019	2.05	1.8	0.578	12.2	7.3	0.1	817
Mb20	1.27	6640	3.49	1.413	3.210	0.024	0.018	2.05	1.8	0.588	14.0	7.5	0.1	816
Mb21	1.29	6637	3.49	1.416	2.655	0.024	0.017	1.95	1.8	0.602	22.1	8.8	0.1	815

Model Mb19 not only has the minimum $\chi^2_{\rm c}$ + $\chi^2_{\nu_{\rm corr}}$ when $\delta_{\rm ov}$ is in the range of $1.7-1.8$, it also reproduces the observed ratios. This shows that the structure of model Mb19 is similar to that of KIC 11081729, and KIC 11081729 may have a large overshoot of convective core. The mass, radius, and age of KIC 11081729 estimated from models with the large $\delta_{\rm ov}$ and with $\chi^2_{\rm c} < 1.0$ and $\chi^2_{\nu_{\rm corr}} < 10.0$ are $1.24 \pm 0.03\ M_\odot$, $1.40 \pm 0.01\ R_\odot$, and 3.6 ± 0.7 Gyr, respectively. The mass and radius are close to those estimated by Metcalfe et al. (2014). But the age is larger than that determined by Metcalfe et al. (2014), which is due to the fact that overshooting of convective core brings more H-rich material into the region of hydrogen burning.

The value of $\chi^2_{\nu_{\rm corr}}$ of Mb19 is larger than that of Mb8. Moreover, the effective temperature and [Fe/H] determined by Molenda-Zakowicz et al. (2013) and Ammons et al. (2006) are different from those estimated by Bruntt et al. (2012). The determination of atmospheric parameters can be affected by spectroscopic methods (Molenda-Zakowicz et al. 2013). Thus we calculated the models with the effective temperature and [Fe/H] determined by Molenda-Zakowicz et al. (2013) and Ammons et al. (2006).

Table 4. Parameters of the models with the effective temperture and [Fe/H] determined by Molenda-Zakowicz et al. (2013). The symbol X_c represents the central hydrogen abundance of models, while ν_0^m indicates the adiabatic oscillation frequency at which the r_{01} of models reaches a minimum.

Model	M ($M_\odot$)	$T_{\rm eff}$ (K)	L ($L_\odot$)	R ($R_\odot$)	age (Gyr)	Z_i	$(Z/X)_s$	α	$\delta_{\rm ov}$	X_c	χ^2_ν	$\chi^2_{\nu_{corr}}$	χ^2_c	ν_0^m (μHz)
Mm1	1.17	6291	2.74	1.393	6.738	0.030	0.029	1.95	1.7	0.524	8.8	8.3	1.0	819
Mm2	1.19	6326	2.82	1.400	6.070	0.030	0.028	1.95	1.7	0.533	8.5	8.0	0.8	818
Mm3	1.21	6403	2.99	1.406	5.564	0.030	0.029	2.05	1.7	0.537	8.5	7.7	0.7	818
Mm4	1.23	6476	3.15	1.413	4.707	0.028	0.026	2.05	1.7	0.553	8.3	7.6	0.5	818
Mm5	1.25	6509	3.24	1.416	4.180	0.028	0.025	2.05	1.7	0.563	8.4	7.3	0.6	817
Mm6	1.27	6543	3.33	1.421	3.706	0.028	0.025	2.05	1.7	0.572	8.4	6.9	0.8	817
Mm7	1.29	6535	3.35	1.429	3.527	0.030	0.027	2.05	1.7	0.575	7.6	6.7	0.9	817
Mm8	1.17	6389	2.89	1.390	6.048	0.026	0.023	1.95	1.8	0.539	10.5	8.4	0.2	818
Mm9	1.19	6423	2.98	1.396	5.421	0.026	0.023	1.95	1.8	0.549	10.6	8.2	0.2	818
Mm10	1.21	6457	3.08	1.403	5.296	0.028	0.025	2.05	1.8	0.546	8.6	7.9	0.5	818
Mm11	1.23	6489	3.17	1.409	4.773	0.028	0.025	2.05	1.8	0.556	8.5	7.8	0.5	818
Mm12	1.25	6441	3.11	1.417	4.388	0.030	0.027	1.95	1.8	0.564	8.8	7.6	0.6	817
Mm13	1.27	6515	3.26	1.419	3.607	0.028	0.024	1.95	1.8	0.579	11.0	7.1	0.5	816
Mm14	1.29	6466	3.19	1.425	3.256	0.030	0.026	1.85	1.8	0.588	12.1	7.1	0.5	816

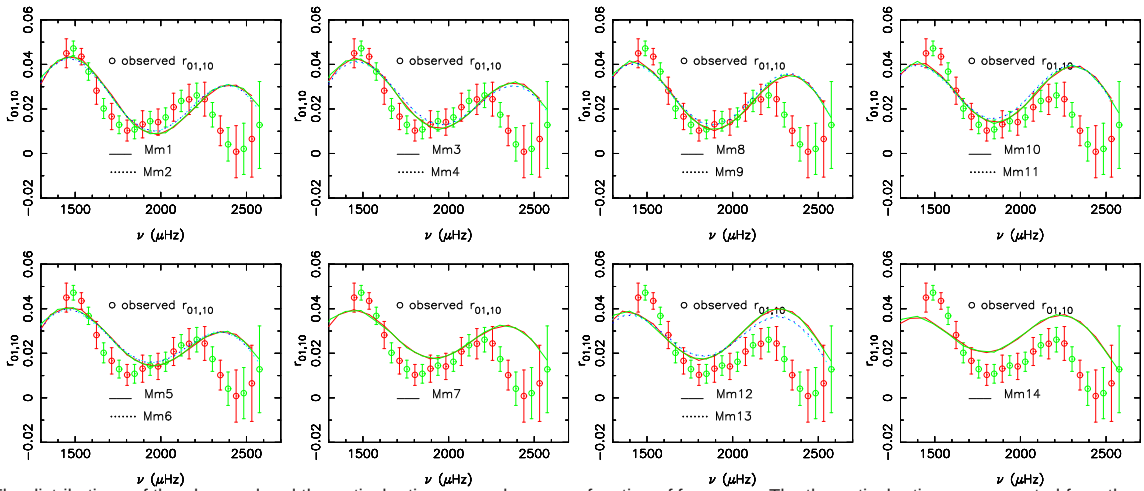

Fig. 4. The distributions of the observed and theoretical ratios r_{10} and r_{01} as a function of frequency. The theoretical ratios are computed from the corrected frequencies $\nu_{\rm corr}$ of the models listed in Table 4.

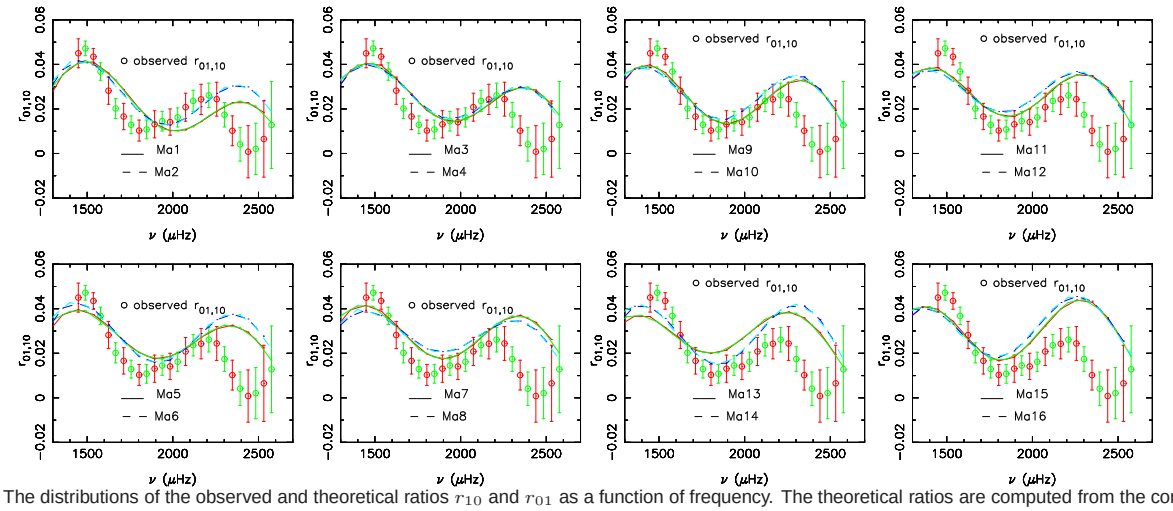

Fig. 5. The distributions of the observed and theoretical ratios r_{10} and r_{01} as a function of frequency. The theoretical ratios are computed from the corrected frequencies $\nu_{\rm corr}$ of the models listed in Table 5.

2.3.2 The models with the effective temperature and [Fe/H] of Molenda-Zakowicz

Table 4 lists the models that minimize $\chi^2_{\rm c} + \chi^2_{\nu_{\rm corr}}$ for a given mass and $\delta_{\rm ov}$. The calculations show that the models with $\delta_{\rm ov} < 1.7$ can not reproduce the observed ratios. Thus we do not considere these models when we estimate the mass and age of KIC 11081729. When the value of $\delta_{\rm ov}$ increases to 1.8, the observed ratios can be reproduced by models (see Figure 4). This indicates that the distributions of ratios r_{10} and r_{01} are mainly dependent on the effects of overshooting of convective core rather than on other effects.

The mass, radius, and age estimated from the models with $\delta_{\rm ov}$ in the range of $1.7 - 1.8$ and with $\chi^2_{\rm c} < 1.0$ and $\chi^2_{\nu_{\rm corr}} < 10.0$ are $1.230 \pm 0.035\ M_{\odot}$, $1.40 \pm 0.01\ R_{\odot}$, and 4.6 ± 0.9 Gyr, respectively. The age of these models are larger than that of models with the effective temperature and [Fe/H] of Bruntt et al. (2012). Thus spectroscopic results can affect the estimation of age of stars. The values of $\chi^2_{\nu_{\rm corr}}$ of these models are as large as those of the models with the effective temperature and [Fe/H] of Bruntt et al. (2012). Thus these models are not better than the models with the effective temperature and [Fe/H] of Bruntt et al. (2012).

2.3.3 The models with the effective temperature and [Fe/H] of Ammons

The effective temperature determined by Ammons et al. (2006) is between that estimated by Molenda-Zakowicz et al. (2013) and that determined by Bruntt et al. (2012). Table 5 lists the models that minimize $\chi^2_{\rm c} + \chi^2_{\nu_{\rm corr}}$ for a given mass and $\delta_{\rm ov}$. The distributions of r_{10} and r_{01} of models with $\delta_{\rm ov}$ less than 1.7 are also not consistent with those of the observed ratios. When the value of $\delta_{\rm ov}$ is in the range of $1.7 - 1.8$, the observed ratios are reproduced well by the models with the large $\delta_{\rm ov}$ (see Figure 5).

Tables $1 - 5$ show that model Ma6 has the minimum $\chi^2_{\rm c} + \chi^2_{\nu_{\rm corr}}$ in the calculations. Moreover, the observed ratios are reproduced by Ma6. Thus Ma6 is the best-fit model in the calculations. When

Table 5. Parameters of the models with the effective temperture and [Fe/H] determined by Ammons et al. (2006). The symbol X_c represents the central hydrogen abundance of models, while ν_0^m indicates the adiabatic oscillation frequency at which the r_{01} of models reaches a minimum.

Model	M ($M_\odot$)	$T_{\rm eff}$ (K)	L ($L_\odot$)	R ($R_\odot$)	age (Gyr)	Z_i	$(Z/X)_s$	α	$\delta_{\rm ov}$	X_c	χ^2_ν	$\chi^2_{\nu_{corr}}$	χ^2_c	ν_0^m (μHz)
Ma1	1.21	6529	3.20	1.400	4.567	0.024	0.020	2.05	1.7	0.557	10.6	8.1	0.7	818
Ma2	1.23	6476	3.15	1.413	4.707	0.028	0.026	2.05	1.7	0.553	8.3	7.6	0.9	818
Ma3	1.25	6509	3.24	1.416	4.180	0.028	0.025	2.05	1.7	0.563	8.4	7.3	0.5	817
Ma4	1.27	6543	3.33	1.421	3.706	0.028	0.025	2.05	1.7	0.572	8.4	6.9	0.4	817
Ma5	1.29	6536	3.35	1.429	3.527	0.030	0.027	2.05	1.7	0.575	7.6	6.7	0.3	817
Ma6	1.30	6597	3.52	1.439	4.209	0.034	0.051	2.15	1.7	0.554	5.5	4.8	0.7	814
Ma7	1.32	6630	3.61	1.442	3.735	0.034	0.051	2.15	1.7	0.563	5.1	4.6	0.9	814
Ma8	1.34	6592	3.54	1.444	2.939	0.034	0.051	1.95	1.7	0.583	10.9	6.4	0.7	814
Ma9	1.21	6542	3.22	1.398	4.631	0.024	0.020	2.05	1.8	0.559	10.8	7.8	0.7	818
Ma10	1.23	6490	3.15	1.406	4.296	0.026	0.022	1.95	1.8	0.568	11.6	7.7	0.9	817
Ma11	1.25	6562	3.32	1.413	3.934	0.026	0.022	2.05	1.8	0.572	10.0	7.2	0.5	817
Ma12	1.27	6515	3.26	1.419	3.607	0.028	0.024	1.95	1.8	0.579	11.0	7.1	0.6	816
Ma13	1.29	6507	3.28	1.426	3.424	0.030	0.026	1.95	1.8	0.582	9.0	7.0	0.5	816
Ma14	1.30	6504	3.31	1.435	5.298	0.026	0.036	1.95	1.8	0.599	7.4	5.7	0.3	815
Ma15	1.32	6487	3.32	1.443	5.054	0.028	0.039	1.95	1.8	0.602	6.5	5.8	0.5	815
Ma16	1.34	6476	3.33	1.451	4.724	0.030	0.042	1.95	1.8	0.604	6.0	5.8	0.7	814
Ma11b	1.25	6522	3.26	1.415	4.240	0.028	0.025	2.05	1.8	0.565	8.5	7.4	0.5	817

the value of $\delta_{\rm ov}$ is equal to 1.8, models Ma14 has the minimum $\chi^2_{\rm c}$ + $\chi^2_{\nu_{\rm corr}}$. Figure 5 shows that the ratios of model Ma14 is almost consistent with the observed ones. Therefore, Ma14 is chosen as the best-fit model for $\delta_{\rm ov}$ = 1.8.

The mass, radius, and age estimated from the models with $\delta_{\rm ov}$ in the range of $1.7-1.8$ and with $\chi^2_{\rm c} < 1.0$ and $\chi^2_{\nu_{\rm corr}} < 10.0$ are $1.270 \pm 0.035\ M_\odot$, $1.420 \pm 0.015\ R_\odot$, and 3.8 ± 0.7 Gyr, respectively. The median age of 3.8 Gyr is larger than the ages of models with $M = 1.27\ M_\odot$ listed in Table 5. This is related to the fact that the table only lists part of the sample. For example, models Ma11 and Ma11b have the same mass and $\chi^2_{\rm c}$, and almost the same $\chi^2_{\nu_{\rm corr}}$, r_{10} and r_{01} (see Figure 6), however, they have different age.

The calculations show that the estimated mass and age rely on spectroscopic results but the

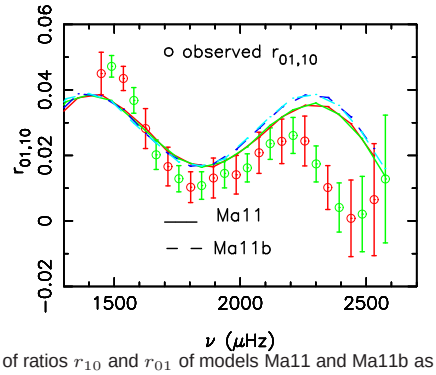

Fig. 6. The distributions of ratios r_{10} and r_{01} of models Ma11 and Ma11b as a function of frequency.

distributions of r_{10} and r_{01} are mainly dependent on the effects of overshooting of convective core. The estimation of $\delta_{\rm ov}$ is not affected by the difference in the spectroscopic results. KIC 11081729 may have a large overshooting of the convective core.

3 Fitting equation for the observed and theoretical ratios

The distributions of r_{10} and r_{01} are dependent on $\delta_{\rm ov}$, which may provide an opportunity to diagnose the size of convective core from observed frequencies.

By making use of the asymptotic formula of frequencies, one can get (Liu et al. 2014)

$$r_{10}(\nu_{n,1}) \simeq 2\nu_{n,1}^{-1} A_0 \Delta\nu, \tag{6}$$

where

$$A_0\Delta\nu = \frac{1}{4\pi^2}[\frac{c(R)}{R} + \int_{r_t}^{R}(-\frac{1}{r}\frac{dc}{dr})dr]. \tag{7}$$

In this equation, c is the adiabatic sound speed at radius r and R is the fiducial radius of the star; r_t is the inner turning point of the mode with the frequency $\nu_{n,1}$. Equation (6) indicates that ratio r_{10} is dependent on the quantity $A_0\Delta\nu$ that is sensitive to the changes in the adiabatic sound speed c. Figure 7 shows that the changes can directly affect the quantity $A_0\Delta\nu$. These hint to us that ratios r_{10} and r_{01} of stars with a convective core could be affected by the changes in the sound speed.

The p-mode oscillations of stars are considered to be acoustic standing waves. The variation with time t of a standing wave is proportional to $\cos(\omega t)$, where the ω is angular frequency. The variation of the modes that penetrate into overshooting region can be affected by convection. For $l = 1$ modes, there should be a critical angular frequency ω_0. When the angular frequency of modes is larger than ω_0, the modes penetrate into overshooting region. We assume that the variation with time of the acoustic wave that is affected by convection is related to $-A\cos(\omega_0 t)$, where A is a free parameter. Due to the fact that oscillation frequencies of stars can be observed, thus we want to know that the effects of convection core on the characteristics of oscillations vary with frequency rather than

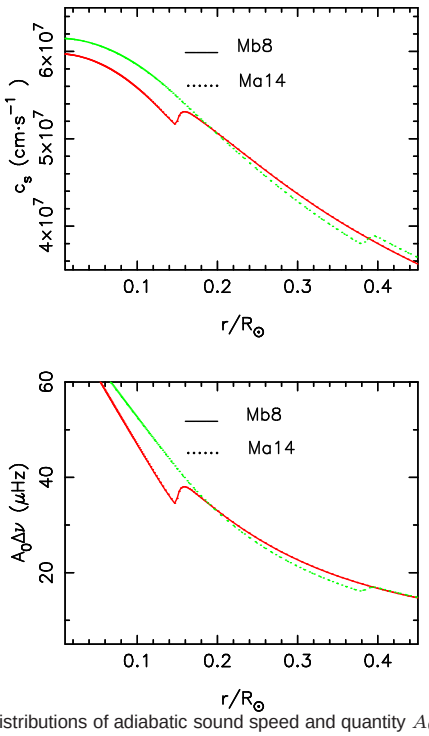

Fig. 7. Radial distributions of adiabatic sound speed and quantity $A_0\Delta\nu$ of models.

with time. This can be achieved by making use of Fourier transform. Thus one can obtain

$$\begin{aligned} B(\omega) &= \tfrac{2}{\pi}\int_0^{2N\pi/\omega_0}[-A\cos(\omega_0 t)\cos(\omega t)]dt \\ &= -\tfrac{A}{\pi}\big[\tfrac{\sin(\frac{2N\pi\omega}{\omega_0})}{\omega+\omega_0}+\tfrac{\sin(\frac{2N\pi\omega}{\omega_0})}{\omega-\omega_0}\big] \\ &= \tfrac{2A\omega}{\pi(\omega_0^2-\omega^2)}\sin(\tfrac{2N\pi\omega}{\omega_0}), \end{aligned} \tag{8}$$

where N is an integer. Taken N as 1 and $\omega_{n,1}=2\pi\nu_{n,1}$, equation (8) can be rewritten as

$$B(\nu_{n,1}) = \frac{2A\nu_{n,1}}{2\pi^2(\nu_0^2-\nu_{n,1}^2)}\sin(\frac{2\pi\nu_{n,1}}{\nu_0})+B_0, \tag{9}$$

where B_0 is a constant. The effects of convection core on the characteristics of oscillations should be shown by function $B(\nu_{n,1})$.

The value of $B(\nu_{n,1})$ reaches maxima at around $3\nu_0/8$ and $7\nu_0/4$, but reaches minima at around ν_0 and $9\nu_0/4$. Thus the value of $B(\nu_{n,1})$ decreases with frequency between about $3\nu_0/8$ and ν_0, but increases with frequency between about ν_0 and $7\nu_0/4$. The value of $B(\nu_{n,1})$ decreases firstly and then increases with frequency in the range of about $7\nu_0/4-11\nu_0/4$. These characteristics are consistent with those of r_{10} and r_{01} calculated from models with a convective core. Thus the ratios r_{10} and r_{01} of stars with a convective core could be described by equation (9).

The observed ratios of KIC 11081729 decrease firstly and then increase with frequency and have a minimum between 1804 and 1846 μHz. Thus one can estimate the value of ν_0 is between about 800 and 820 μHz. Due to the fact that the value of $\sin(2\pi\nu_{n,1}/\nu_0)$ is 0 at $\nu_0/2$ and $3\nu_0/2$, hence B_0 is not a free parameter. For a given ν_0, the value of B_0 takes the value of ratio r_{10} or r_{01} at $\nu_0/2$

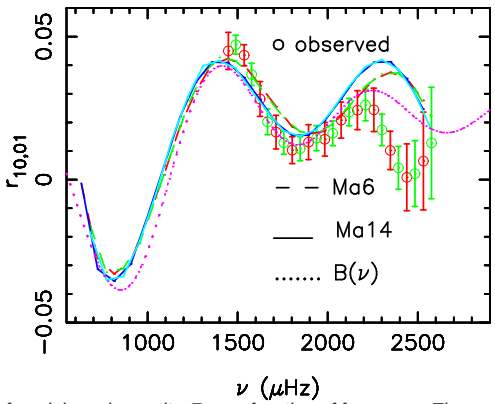

Fig. 8. The distributions of ratios r_{10} and r_{01} of models and quantity B as a function of frequency. The quantity B is computed by using equation (9) with $A = 50\pi$, $B_0 = 0.023$, and $\nu_0 = 820$ μHz

.

or $3\nu_0/2$. Thus we obtained the value of B_0 is between 0.019 and 0.026 from the ratios of Ma6. In addition, using equation (9) and the observed $\nu_{n,1}$ and r_{10}, the values of parameters A, B_0, and ν_0 are estimated to be 53 ± 21 π, 0.018 ± 0.003, and 795 ± 21 μHz,respectively. Figure 8 shows that the ratios of KIC 11081729 are reproduced well by equation (9) with $A = 50\pi$, $B_0 = 0.023$, and $\nu_0 = 820$ μHz. The distributions of r_{10} and r_{01} of Ma6 and Ma14 are reproduced well by equation (9). The ratios r_{10} and r_{01} of models Ma6 and Ma14 reach the minimum at about 810 μHz that are consistent with 795 ± 21 μHz estimated by using equation (9).

3.1 Test the equation by other stars

Tian et al. (2014) studied the oscillations of KIC 6225718, and determined that the mass of KIC 6225718 is $1.10^{+0.04}_{-0.03}$ $M_\odot$, but could not determine whether a convective core exists in KIC 6225718. From observed frequencies, one can obtain $A = 745 \pm 527$ π, $B_0 = 0.021 \pm 0.008$, and $\nu_0 = 5700 \pm 423$ μHz for KIC 6225718. The panel (a) of Figure 9 shows that the observed ratios of KIC 6225718 are reproduced well by equation (9) with $A = 745$ π, $B_0 = 0.021$, and $\nu_0 = 5700$ μHz. Using equation (16) of Liu et al. (2014) with $f_0 = 2$, the value of ν_0 for the best model 14 of KIC 6225718 (Tian et al. 2014) is estimated to be 5890 μHz. According to equation (9), ratios r_{10} and r_{01} reach the minimum at around ν_0. The ratios r_{10} and r_{01} calculated from the model 14 reach the minimum at 5642 μHz. The two values are consistent with 5700 ± 423 μHz. The ratios of KIC 6225718 mainly exhibit a decreasing behavior. But the observed ratios have a maximum at about 1926 μHz, which is consistent with that $B(\nu)$ has a maximum at around $3\nu_0/8$. The model 14 has a small convective core and $\delta_{\rm ov} = 0.2$ (Tian et al. 2014). These indicate that a small convective core may exist in KIC 6225718. The value of $\nu_{\rm max}$ of KIC 6225718 is 2031 μHz that is much less than the value of ν_0 (5700 ± 423 μHz).

The values of A, B_0, and ν_0 computed from the observed frequencies of HD 49933 (Benomar

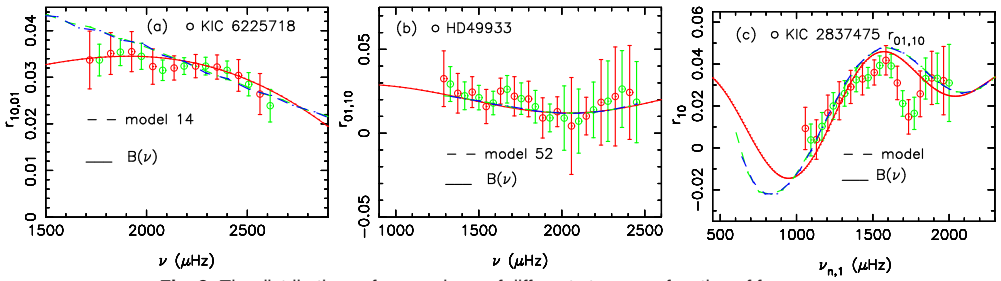

Fig. 9. The distributions of r_{10} and r_{01} of different stars as a function of frequency.

et al. 2009) are 54 ± 14 π, 0.040 ± 0.006, and 1920 ± 46 μHz. Using equation (16) of Liu et al. (2014) with $f_0 = 2$, the value of ν_0 for model M52 of HD 49933 (Liu et al. 2014) is estimated to be about 1900 μHz. The ratios of model M52 reach the minimum at about 2057 μHz. The panel (b) of Figure 9 shows that the ratios of model M52 are consistent with those computed by equation (9) with $A = 31$ π, $B_0 = 0.028$, and $\nu_0 = 1966$ μHz. The model M52 has a large convective core and $\delta_{\rm ov}$ $= 0.7$ (Liu et al. 2014). The value of $\nu_{\rm max}$ of HD 49933 is 1760 μHz (Appourchaux et al. 2008) that is close to 1920 ± 46 μHz of ν_0. The values of extracted frequencies of HD 49933 are in the vicinity of ν_0. The ratios of HD 49933 decrease and then increase with frequency, which is consistent with that calculated from equation (9).

Moreover, the panel (c) of Figure 9 shows that the observed and theoretical ratios of KIC 2837475 are reproduced by equation (9) with $A = 43$ π, $B_0 = 0.033$, and $\nu_0 = 913$ μHz in the range of about $1000 - 2000$ μHz. The values of ν_0 computed from the observed frequencies of KIC 2837475 is 913 ± 36 μHz. The ratios r_{10} and r_{01} calculated from model Ma14 of KIC 2837475 (Yang et al. 2015) reach the minimum at about 850 μHz. The model has a large convective core and $\delta_{\rm ov} = 1.4$ (Yang et al. 2015). The value of $\nu_{\rm max}$ of KIC 2837475 is 1522 μHz that is much larger than 913 ± 36 μHz of ν_0. The values of extracted frequencies of KIC 2837475 are in the range between about ν_0 and $9\nu_0/4$. The ratios of KIC 2837475 increase and then decrease with frequency, which is also consistent with that calculated from equation (9).

The distributions of r_{10} and r_{01} of different stars with a convective core can be reproduced well by equation (9). The value of $\nu_{\rm max}$ of KIC 6225718 is less than the value of ν_0. KIC 6225718 may have a small convective core and a small $\delta_{\rm ov}$. The value of $\nu_{\rm max}$ of HD 49933 is close to the value of ν_0. HD 49933 may have a medium $\delta_{\rm ov}$. The value of $\nu_{\rm max}$ of KIC 2837475 and KIC 11081729 is larger than that of ν_0, respectively. KIC 2837475 and KIC 11081729 may have a large $\delta_{\rm ov}$. The equation (9) could be used to determine the presence of convective core and estimate the size of overshoot from observed frequencies.

4 DISCUSSION AND SUMMARY

4.1 Discussion

Mazumdar et al. (2014) showed that ratios r_{10} and r_{01} can be affected by the glitches at the BCZ and the layers of the HeIIZ. The changes in frequencies caused by the glitch at the BCZ or the layers of the HeIIZ have a periodicity of twice the acoustic depth of the corresponding glitch (Mazumdar et al. 2014). The value of the acoustic depth τ_{HeIIZ} and τ_{BCZ} is about 720 and 2060 s for model Mb8, respectively. The value of τ_{HeIIZ} and τ_{BCZ} of model Mb19 is 728 and 2100 s, respectively. The values of τ_{HeIIZ} and τ_{BCZ} of model Mb8 are approximately equal to those of model Mb19. Thus the glitches should result in a similar effect on the ratios of models Mb8 and Mb19. However, the distributions of ratios r_{10} and r_{01} of model Mb8 are obviously different from those of model Mb19. Thus, the difference between the ratios of Mb8 and those of Mb19 (see Figures 2 and 3) does not derive from the effects of the glitch at the BCZ or the HeIIZ.

For different spectroscopic results, only the models with $\delta_{\rm ov}$ in the range of about $1.7-1.8$ can reproduce the observed ratios. This indicates that the uncertainties of the effective temperature and [Fe/H] can not significantly affect the estimation of $\delta_{\rm ov}$. This is due to the fact that the estimation of $\delta_{\rm ov}$ is mainly dependent on the distributions of ratios r_{10} and r_{01} that are only determined by the interior structure (Roxburgh & Vorontsov 2003; Oti Floranes et al. 2005). Tables $2-5$ list the value of adiabatic oscillation frequency ν_0^m at which r_{10} and r_{01} computed from models arrive at the minimum. The values of ν_0^m of models with $\delta_{\rm ov}$ in the range of $1.7-1.8$ are consistent with that determined by equation (9). The calculations show that the value of ν_0^m is related to the radius of overshooting region of models. The larger the radius of the core including the overshooting region, the smaller the value of ν_0^m. For KIC 6225718, HD 49933, KIC 2837475, and KIC 11081729 the values of ν_0 estimated from observed ratios by using equation (9) are consistent with those obtained from r_{10} and r_{01} of the best model of the stars. Thus equation (9) aids in understanding the size of the core from the observed ratios. If the value of ν_{max} of a star is less than the value of ν_0 estimated by using equation (9), the star may have a relatively small convective core. However, if the value of ν_{max} is larger than that of ν_0, the star may have a large convective core.

The value of $1.7-1.8$ of the $\delta_{\rm ov}$ is much larger than the value adopted usually. However, Xiong (1985) shows that the overshooting of convective core could mix material in the distance of $1.4H_p$. Moreover, the value is consistent with the numerical result for the downward overshooting of giants (Tian et al. 2009). A large $\delta_{\rm ov}$ means that an efficient mixing takes place in stellar interior. Rotation can lead to an increase in convective core, which depends on the efficiency of rotational mixing and rotation rate (Maeder 1987; Yang et al. 2013a; Yang et al. 2013b). The effects of rotation

explain the extended MS turnoffs of intermediate-age star clusters in the Large Magellanic Cloud, where rotational mixing plays an important role (Yang et al. 2013b). The effects of rotational mixing and convection overshoot can reconcile the low-Z solar models with helioseismology (Yang 2016). Efficient mixing and convection overshoot also may exist in the Sun (Yang 2016). The effect of overshooting can mimic the effects of rotational mixing to a certain degree. The surface rotation period of KIC 11081729 is about 2.78 days (McQuillan et al. 2014), which is obviously lower than the approximately 27 days of the Sun. The large $\delta_{\rm ov}$ might be related to rotation.

4.2 Summary

The observed ratios r_{10} and r_{01} of KIC 11081729 decrease firstly and then increase with frequency. There are different spectroscopic results for KIC 11081729, which can affect the determinations of mass and age of KIC 11081729 but can not affect the estimation of $\delta_{\rm ov}$. This is due to the fact that the distributions of r_{10} and r_{01} are mainly dependent on the interior structure. The structure can be directly changed by overshooting of convective core. Thus the distributions of r_{10} and r_{01} are sensitive to $\delta_{\rm ov}$. For the different spectroscopic constraints, the models with $\delta_{\rm ov}$ less than 1.7 can not reproduce the observed ratios. However, the distributions of the observed ratios can be reproduced well by models with $\delta_{\rm ov}$ in the range of about $1.7-1.8$. A large overshooting of convective core may exist in KIC 11081729. The behavior of the ratios of KIC 11081729 may derive from the effects of the large overshooting of convective core.

The ratios r_{10} and r_{01} calculated from models with a convective core reach a minimum at about ν_0, arrive at a maximum at around $7\nu_0/4$, and then reach a minimum at about $9\nu_0/4$. These characteristics can be completely reproduced by equation (9). The distributions of observed and theoretical ratios of stars with a convective core can be reproduced well by the equation. The value of ν_0 decreases with the increase in the radius of convective core and can be estimated by formula (9) from observed frequencies. Thus the equation aids in determining the presence and the size of convective core including overshooting region from observed frequencies. If the value of ν_{max} of a star is less than the value of ν_0 determined from observed frequencies using equation (9), the star may have a small convective core and a small $\delta_{\rm ov}$. However, if the value of ν_{max} is larger than that of ν_0, the star may have a large overshooting of convective core.

Acknowledgments

The author acknowledges the support from the NSFC 11273012, 11273007, 11503039, and the HSCC of Beijing Normal University.

References

Alexander, D. R., Ferguson, J. W. 1994, ApJ, 437, 879

Ammons, S. M., Robinson, S. E., Strader, J., Laughlin, G., Fischer, D., & Wolf, A. 2006, ApJ, 638, 1004

Anders, E, & Grevesse, N. 1989, Geochim. Cosmochim. Acta, 53, 197

Appourchaux, T., Chaplin, W. J., García, R. A., et al. 2012, A&A, 543, A54

Appourchaux, T., Michel, E., Auvergne, M., et al. 2008, A&A, 488, 705

Asplund, M., Grevesesse N., Sauval, A. J., Allende Prieto, C., & Blomme, R., 2005, A&A, 431, 693

Benomar, O., Baudin, F., Campante, T. L., et al. 2009, A&A, 507, L13

Bond, H. E., Gilliland, R. L., Schaefer, G. H. et al. 2015, ApJ, 813, 106

Bruntt, H., Basu, S., Smalley, B., et al. 2012, MNRAS, 423, 122

Chaplin, W. J., Basu, S., Huber, D., et al. 2014, ApJS, 210, 1

Christensen-Dalsgaard, J., & Houdek, G. 2010, Ap&SS, 328, 51

Cunha, M. S., & Metcalfe, T. S. 2007, ApJ, 666, 413

Demarque, P., Sarajedini, A., Guo, X.-J. 1994, ApJS, 426, 165

De Meulenaer, P., et al. 2010, A&A, 523, A54

Deheuvels, S., Bruntt, H., Michel, E., et al. 2010, A&A, 515, A87

Droege, T. F., Richmond, M. W., Sallman, M. P., Creager, R. P. 2006, PASP, 118, 1666

Flower, P. J. 1996, ApJ, 469, 355

Gough, D. O., & Thompson, M. J. 1988, in IAU Symp. 123, Advances in Helio- and Asteroseismology, ed. J. Christensen-Dalsgaard & S. Frandsen (Dordrecht: Reidel), 15

Grevesse, N., & Sauval, A. J. 1998, in Solar Composition and Its Evolution, ed. C. Fröhlich et al. (Dordrecht: Kluwer), 161

Guenther, D. B. 1994, ApJ, 422, 400

Guenther, D. B., Demarque, P., & Gruberbauer, M., 2014, ApJ, 787, 164

Huber, D., Silva Aguirre, V., Matthews, J. M., et al. 2014, ApJS, 211, 2

Iglesias, C., Rogers, F. J. 1996, ApJ, 464, 943

Kjeldsen, H., Bedding, T. R., & Christensen-Dalsgaard, J. 2008, ApJL, 683, L175

Liu, Z., Yang, W., Bi, S., et al. 2014, ApJ, 780, 152

Maeder, A., 1987, A&A, 178, 159

Mazumdar, A., Basu, S., Collier, B. L., & Demarque, P. 2006, MNRAS, 372, 949

Mazumdar, A., Monteiro, M. J. P. F. G., Ballot, J., et al. 2014, ApJ, 782, 18

McQuillan, A., Mazeh, T., Aigrain, S. 2014, ApJS, 211, 24

Metcalfe, T. S., Creevey, O. L., Doğan, G., et al. 2014, ApJS, 214, 27

Molenda-Zakowicz, J., Sousa, S. G., Frasca, A., et al. 2013, MNRAS, 434, 1422

Oti Floranes, H., Christensen-Dalsgaard, J., & Thompson, M. J. 2005, MNRAS, 356, 671

Pickles, A., & Depagne, *É*. 2010, PASP, 122, 1437

Pinsonneault, M. H., Kawaler, S. D., Sofia, S., & Demarqure, P. 1989, ApJ, 338, 424

Pinsonneault, M. H., An, D., Molenda-Zakowicz, J., Chaplin, W. J., Metcalfe, T. S., Bruntt, H. 2012, ApJS, 199, 30

Prather, M. J., & Demarque, P. 1974, ApJ, 193, 109

Rogers, F. J., & Nayfonov, A. 2002, ApJ, 576, 1064

Roxburgh, I. W., & Vorontsov, S. V. 2003, A&A, 411, 215

Schröder K. P., Pols O. R., Eggleton P. P. 1997, MNRAS, 285, 696

Silva Aguirre, V., Basu, S., Brandao, I. M., et al. 2013, ApJ, 769, 141

Spergel, D. N., Bean, R., Dore, O., et al., 2007, ApJS, 170, 377

Thoul, A. A., Bahcall, J. N., Loeb, A. 1994, ApJ, 421, 828

Tian, C. L., Deng, L. C., & Chan, K. L. 2009, MNRAS, 398, 1011

Tian, Z. J., Bi, S. L., Yang, W. M., et al. 2014, MNRAS, 445, 2999

Turcotte, S., Richer, J., & Michaud, G. 1998, ApJ, 504, 559

Valle, G., Dell'Omodarme, M., Prada Moroni, P. G., Degl'Innocenti, S. 2016, A&A (arXiv:1601.01535)

Wright, C. O., Egan, M. P., Kraemer, K. E., Price, S. D. 2003, 125, 359

Xiong, D. R. 1985, A&A, 150, 133

Yang, W., & Bi, S. 2007, ApJL, 658, L67

Yang, W., Meng, X., Bi, S., et al. 2012, MNRAS, 422, 1552

Yang, W., Bi, S. & Meng, X. 2013a, RAA, 13, 579

Yang, W., Bi, S. Meng, X., & Liu, Z. 2013b, ApJ, 776, 112

Yang, W., Tian, Z., Bi, S., Ge, Z., Wu, Y., Zhang, J. 2015, MNRAS, 453, 2094

Yang, W. 2016, ApJ, accepted (arxiv:1603.01666)